

TORWARD HYBRID NEOCLASSICAL- MAGNETOHYDRONAMIC SIMULATIONS OF CORE PLASMA INSTABILITIES

B.C. LYONS (PPPL), S.C. JARDIN (PPPL), J.J. RAMOS (MIT PSFC)

CEMM GROUP MEETING
PROVIDENCE, RI
SUNDAY, OCTOBER 28, 2012

Acknowledgements

- This work has been supported by
 - ▣ the U.S. Department of Energy under grant nos. DEFC02-08ER54969 and DEAC02-09CH11466 and the SciDAC Center for Extended Magnetohydrodynamic Modeling (CEMM).
 - ▣ an award from the Department of Energy (DOE) Office of Science Graduate Fellowship Program (DOE SCGF). The DOE SCGF Program was made possible in part by the American Recovery and Reinvestment Act of 2009. The DOE SCGF program is administered by the Oak Ridge Institute for Science and Education for the DOE. ORISE is managed by Oak Ridge Associated Universities (ORAU) under DOE contract number DE-AC05-06OR23100. All opinions expressed in this presentation are the author's and do not necessarily reflect the policies and views of DOE, ORAU, or ORISE.

3

Introduction

How can one model neoclassical tearing modes?

Neoclassical tearing mode modeling

4

- NTM stability place a severe limit on maximum β
- Most common cause of disruptions on JET¹
- High-fidelity simulations required for prediction, control, avoidance, and understanding of NTMs
 - ▣ Especially important for ITER operation, in which very few disruptions can be tolerated²
- NTMs incorporate a lot of physics
 - ▣ Cause: Neoclassical kinetic theory (bootstrap current)
 - ▣ Effect: MHD destabilization (island growth)
 - ▣ Requires a hybrid model

¹ P.C. de Vries, et al., Nucl. Fusion **51**, 053018 (2011)

² T.C. Hender, et al., Nucl. Fusion **47**, S128-S202 (2007)

Framework for hybrid solver

5

- Use existing MHD time-evolution code (e.g., M3D-C¹, NIMROD)
- Desirable traits for neoclassical drift–kinetic equation (DKE) solver
 - Three-dimensional toroidal geometry
 - Study nonaxisymmetric geometries with magnetic islands
 - Full Fokker-Planck-Landau collision operator
 - Use of model collision operators can lead to errors of 5%-10%³
 - Continuum model
 - Good convergence properties, especially for long times
 - Straight-forward coupling to MHD solvers
 - Potentially more computationally efficient than PIC
- No code currently exists that has all of these traits

³ E.A. Belli and J. Candy, Plasma Phys. Control. Fusion **54**, 015015 (2012)

Ramos Form of DKE

6

- J.J. Ramos (Phys. Plasmas 2010 & 2011) provides analytic framework for a neoclassical solver appropriate for core plasma instability simulations
- Velocity taken in frame of each species' macroscopic flow
- Two expansion parameters for high-temperature fusion plasmas

$$\delta \sim \rho_i/L \ll 1 \quad \nu_* \sim L/\lambda_{\text{mfp}} \sim \delta$$

- Maintain equations to lowest order exhibiting collisional dynamics
 - Electron DKE is maintained to order $\delta_e \nu_*$, or δ^3
 - Ion DKE should be maintained to order δ^2
- For now, ion DKE is maintained to order $\delta \nu_*$, with $\delta \ll \nu_* \ll 1$
 - This is conventional neoclassical banana dynamics for both species
- DKE evolves difference between the full distribution function and a shifting Maxwellian (like delta-f)

7

Neoclassical Ion-Electron Solver

NIES solves for the non-adiabatic distribution function to zeroth-order in collisionality in a stationary, axisymmetric toroidal plasma

NIES overview

8

- Work in 4D phase space w/ flux coordinates: $(\psi, \theta, v, \lambda)$
- Distribution function: $\bar{f}_s = (1 + g_{s,0} + g_{s,1} v_{\parallel}) f_{Ms} + h_s$
- Non-adiabatic piece: $h_s = \varsigma(v_{\parallel}) H(1 - \lambda) K_s(\psi, v, \lambda) + h_s^{even}$
 - K_s is independent of θ
 - Dimensionless magnetic moment: $\lambda = \sin^2 \chi B_{max}(\psi) / B(\psi, \theta)$
- DKE reduced to a solvability condition

$$\oint_{\psi, v, \lambda} \frac{dl}{v_{\parallel}} C_s [\varsigma H K_s] = - \oint_{\psi, v, \lambda} dl S_s$$

- Ion source contains ion temperature gradient drive
- Electron source contains ohmic drive, interaction with ion flow, and pressure and electron temperature gradient bootstrap drive
- Need only be solved for passing particles

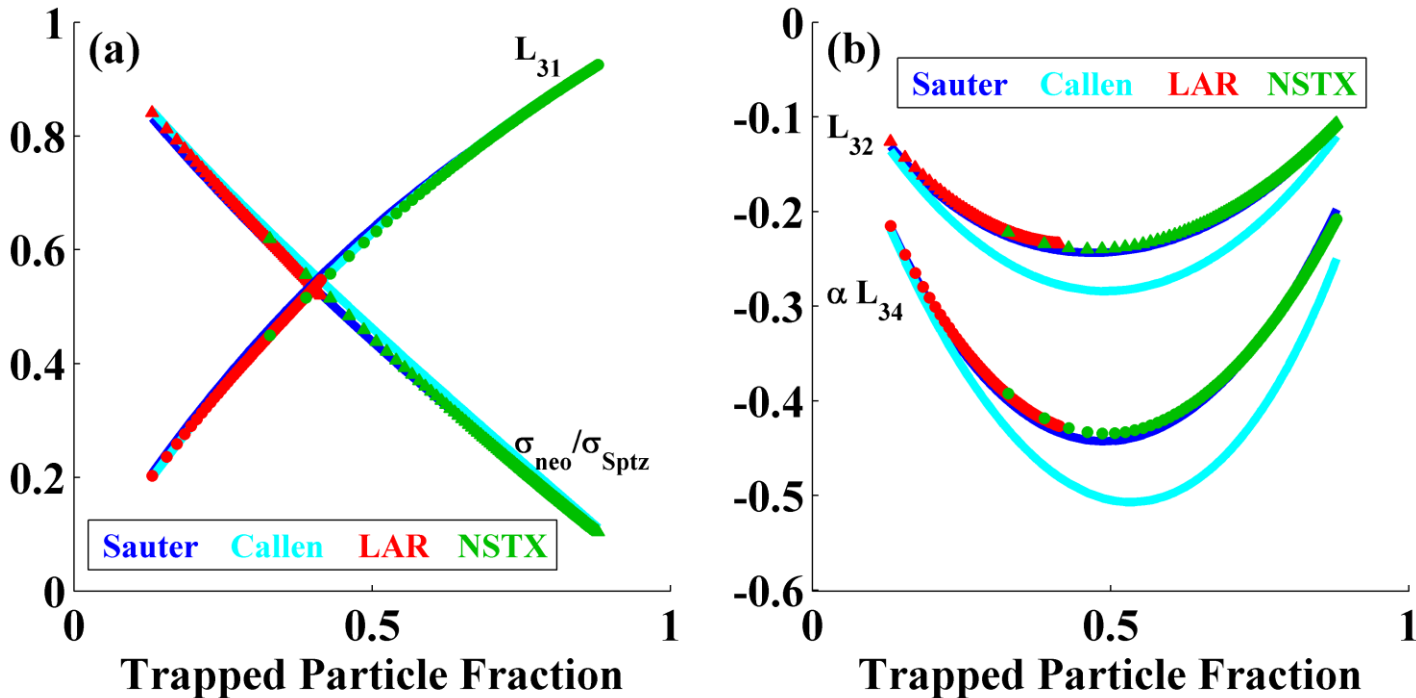
NIES computational methods

9

- Expansions
 - ▣ Expand Rosenbluth Potentials in Legendre polynomials in $y = \cos \chi$, Fourier series in $\cos \theta$, and piecewise linear finite elements in \mathcal{V}
 - ▣ Then expand K_s in piecewise linear finite elements in \mathcal{V} and λ
- Solvability condition and the Rosenbluth Potential Poisson equations solved simultaneously on one flux surface at a time
 - ▣ Inner products taken with finite elements, Legendre polynomials, and Fourier modes
 - ▣ Matrix equation is block tridiagonal in \mathcal{V} , allowing for efficient solution method
 - ▣ Simple moment of K_s gives ohmic and bootstrap current

Benchmarks

10



$$\langle \mathbf{J} \cdot \mathbf{B} \rangle = \sigma_{neo} \langle \mathbf{E} \cdot \mathbf{B} \rangle - cI \left[\mathcal{L}_{31} \frac{dp}{d\psi} + \mathcal{L}_{32} n_e \frac{dT_e}{d\psi} + \mathcal{L}_{34} \alpha n_i \frac{dT_i}{d\psi} \right]$$

- Sauter analytic fits: O. Sauter, et al., Contrib. Plasma Phys. **34**, 2/3, pp 169-174 (1994).
- Callen analytic fomulae: J.D. Callen, et al., Phys. Plasmas **17**, 056113 (2010).
- Our results: B.C. Lyons, S.C. Jardin, and J.J. Ramos, Phys. Plasmas **19**, 082515 (2012).

11

Hybrid Simulations

Axisymmetric case

Overview of next step

12

- Retain axisymmetric geometry for now
- Want to solve the full Ramos DKE without further expansions in collisionality
 - ▣ Extends result to first-order in collisionality
 - ▣ Allows solution to vary poloidally
- Will couple directly to reduced MHD equations

Reduced MHD equations

13

- Use the two field representation

$$\mathbf{B} = \nabla\psi \times \nabla\zeta + I_0 \nabla\zeta \quad \mu_0 \mathbf{J} = -\Delta^* \psi \nabla\zeta \quad \mathbf{u} = R^2 \nabla U \times \nabla\zeta$$

- Combining Faraday's Law and Ohm's law gives

$$\dot{\psi} + R^2 [\psi, U] = \frac{R^2}{en} \mathbf{F}_e^{coll} \cdot \nabla\zeta$$

- ▣ Collisional friction force:

$$\mathbf{F}_e^{coll} = \frac{2m_e \nu_e}{3\sqrt{2\pi}e} \mathbf{J} - 2\pi m_e \nu_e v_{the}^3 \int_0^\infty dv' \int_0^\pi d\chi \sin\chi \cos\chi f_{NM_e} \mathbf{b}.$$

- Momentum equation gives

$$\nabla \cdot (R^2 \nabla \dot{U}) + \frac{1}{2} [R^2 (U, U), R^2] + [R^4 \nabla^2 U, U] = \frac{1}{nm_i} [\Delta^* \psi, \psi]$$

Note that: $(a, b) = \nabla a \cdot \nabla b$. $[a, b] = \nabla\zeta \cdot (\nabla a \times \nabla b)$

$$\Delta^* a = R^2 \nabla_\perp \cdot (R^{-2} \nabla a)$$

Reduced DKE

14

- To start, assume:
 - ▣ Flat and stationary temperature & density profiles
 - ▣ Zero pressure anisotropy
 - ▣ Large aspect ratio
 - ▣ Equal ion and electron temperatures
- DKE simplifies to

$$\frac{\partial f_{NM_e}}{\partial t} + v \cos \chi \mathbf{b} \cdot \nabla f_{NM_e} + \frac{1}{2} v \sin \chi \mathbf{b} \cdot \nabla \ln B \frac{\partial f_{NM_e}}{\partial \chi} = -\frac{v \cos \chi}{n T_e} \mathbf{b} \cdot \mathbf{F}_e^{coll} f_{Me} + \langle C_{ee} + C_{ei} \rangle$$

$$\begin{aligned} \langle C_{ee} + C_{ei} \rangle = & \nu_{De}(v) \mathcal{L}[f_{NM_e}] + \frac{\nu_e v_{the}^3}{v^2} \frac{\partial}{\partial v} \left\{ \xi_e \left[v \frac{\partial f_{NM_e}}{\partial v} + \frac{v^2}{v_{the}^2} f_{NM_e} \right] + \xi_i \left[v \frac{\partial f_{NM_e}}{\partial v} + \frac{m_e v^2}{m_i v_{thi}^2} f_{NM_e} \right] \right\} \\ & + \frac{\nu_e v_{the}}{n} f_{Me} \left(4\pi v_{the}^2 f_{NM_e} - \Phi_e[f_{NM_e}] + \frac{v^2}{v_{the}^2} \frac{\partial^2 \Psi_e[f_{NM_e}]}{\partial v^2} \right) + \nu_e f_{Me} \frac{v_{the}}{v_{thi}^2} \frac{\mathbf{b} \cdot \mathbf{J}}{en} \xi_{iy} \end{aligned}$$

Timescales

15

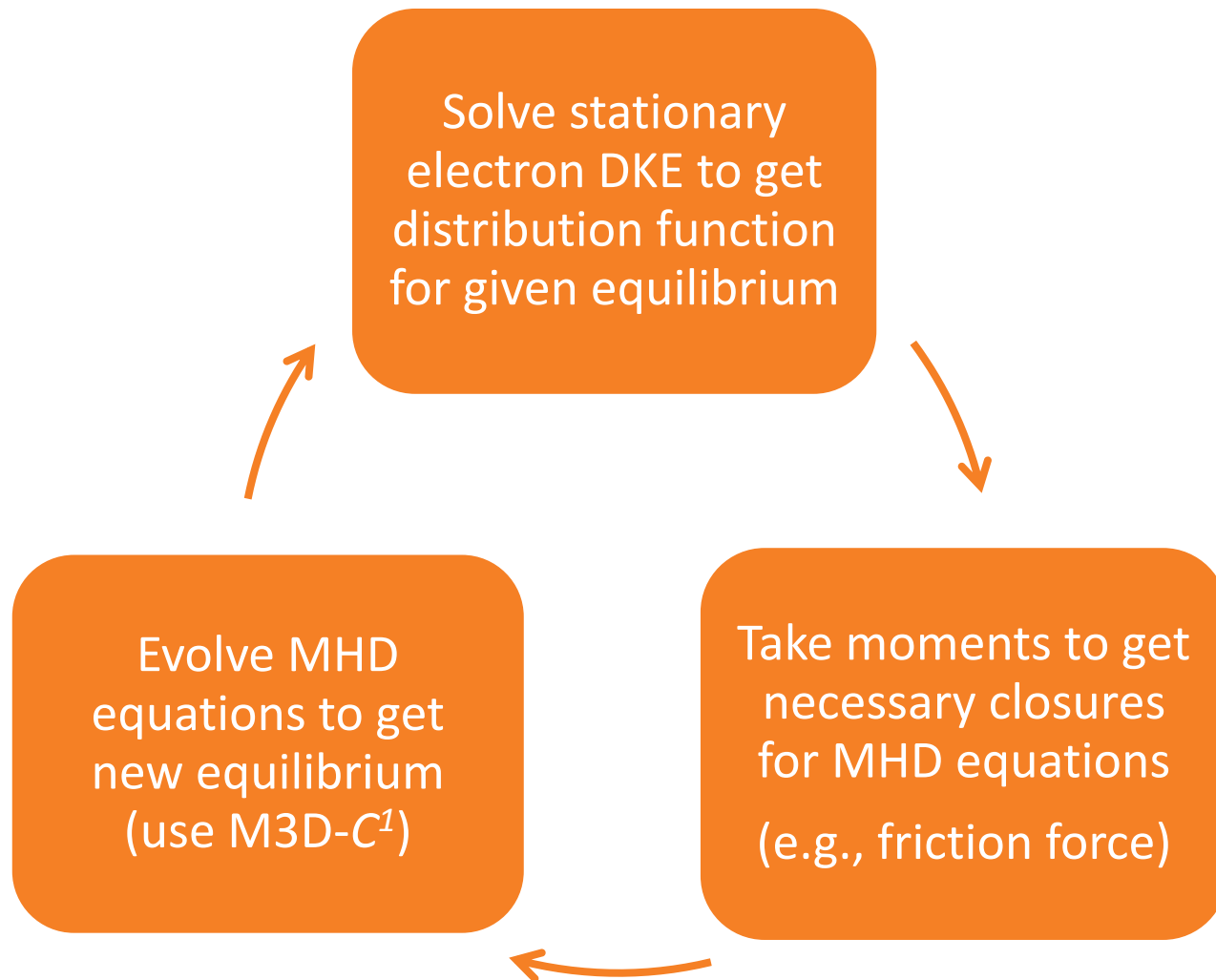
Machine	n (m^{-3})	T (keV)	B (T)	a (m)	R (m)
LTX	3.15×10^{19}	0.2	0.34	0.26	0.4
NSTX	9.04×10^{19}	1	0.45	0.65	0.85
DIII-D	1.13×10^{20}	5	2.1	0.65	1.67
ITER	1.19×10^{20}	20	5.3	2.0	6.2

Machine	τ_{Alfven} (s)	$\tau_{e,conv}$ (s)	$\tau_{i,conv}$ (s)	$\tau_{e,coll}$ (s)	$\tau_{i,coll}$ (s)	$\tau_{resistive}$ (s)
LTX	3.0×10^{-7}	6.7×10^{-8}	2.9×10^{-6}	5.8×10^{-7}	2.5×10^{-5}	3.3×10^{-1}
NSTX	8.2×10^{-7}	6.4×10^{-8}	2.7×10^{-6}	2.0×10^{-6}	8.6×10^{-5}	2.0×10^1
DIII-D	3.9×10^{-7}	5.6×10^{-8}	2.4×10^{-6}	1.6×10^{-5}	6.7×10^{-4}	2.0×10^2
ITER	5.9×10^{-7}	1.0×10^{-7}	4.5×10^{-6}	1.1×10^{-4}	4.6×10^{-3}	1.3×10^4

- Difficult to consider DKE time dependently
 - ▣ In DKE, collision time 10 - 10^3 longer than convective time
 - ▣ MHD resistive time 10^6 - 10^8 longer than collision time
- Reasonable to assume that distribution function evolves to steady state on the resistive timescale

Proposed solution iteration

16



Proposed expansions in DKE

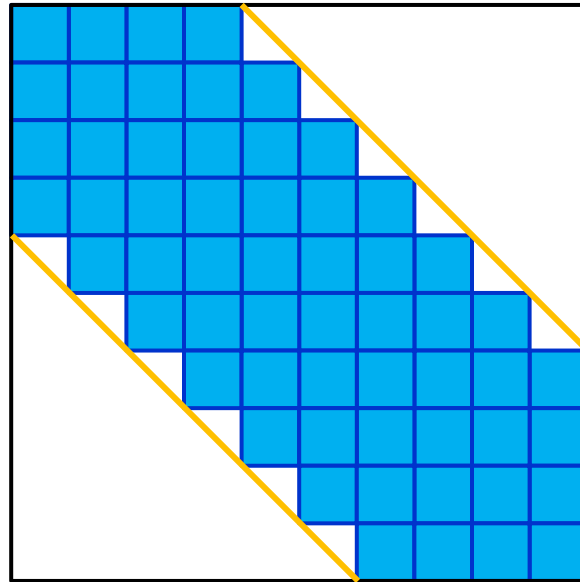
17

- Velocity
 - Cubic B-spline finite elements for v
- Pitch angle
 - λ no longer a good expansion variable
 - Use $y = \cos \chi$ instead
 - Legendre polynomials
 - Finite elements
- Configuration Space
 - (ψ, θ) - only need to expand poloidal angle
 - Fourier modes
 - Finite elements
 - (R, Z) - finite elements

Proposed Solution Method

18

- Cubic B-spline finite elements create block septadiagonal matrix in \mathcal{V}



- Each block contains information on y and θ derivatives
- Solve as a sparse banded matrix using ScaLAPACK

Test problem

19

- Diffusion of current into a toroidal plasma due to a loop voltage at its edge
- Current evolves self-consistently with equilibrium
- Should observe neoclassical conductivity reduction
 - ▣ Trapped particles carry no net current
 - ▣ Can benchmark to theoretical and numerical results
- Code currently in production

Extensions to axisymmetric code

20

- Eventually want to solve time-independent, axisymmetric form of the full Ramos DKE
 - ▣ Allow separate ion and electron temperatures
 - ▣ Relax constraints on density and temperature profiles
 - ▣ Relax large aspect ratio equilibrium assumption
- Will have to solve separate, but similar, ion DKE
- Will allow for simulations of the inductive formation of the bootstrap current
- Use full six-field MHD model with M3D- C^1 to self-consistently evolve pressure as well

21

Conclusion

Summary

22

- The operation of ITER and other future MCF experiments requires predictive capabilities for core plasma instabilities (e.g., Sawtooths, NTMs)
- To date, no neoclassical code exists that is well-suited for such simulations
- We are creating such a code based on the Ramos drift-kinetic formulation
 - ▣ Axisymmetric hybrid code currently in development
 - ▣ Work on nonaxisymmetric code should be underway by next year's APS
 - See my poster (#112 Tuesday afternoon) for more info

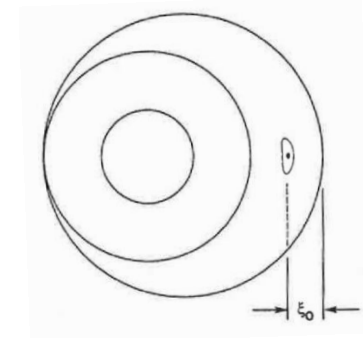
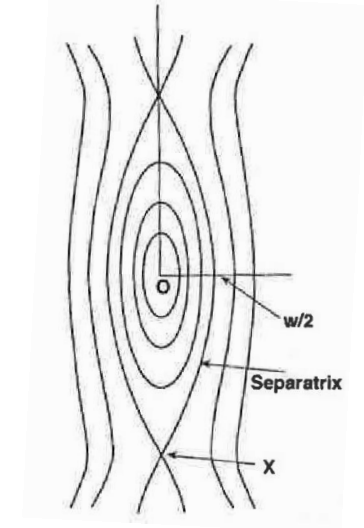
23

Additional Slides

Neoclassical tearing mode (NTMs)

24

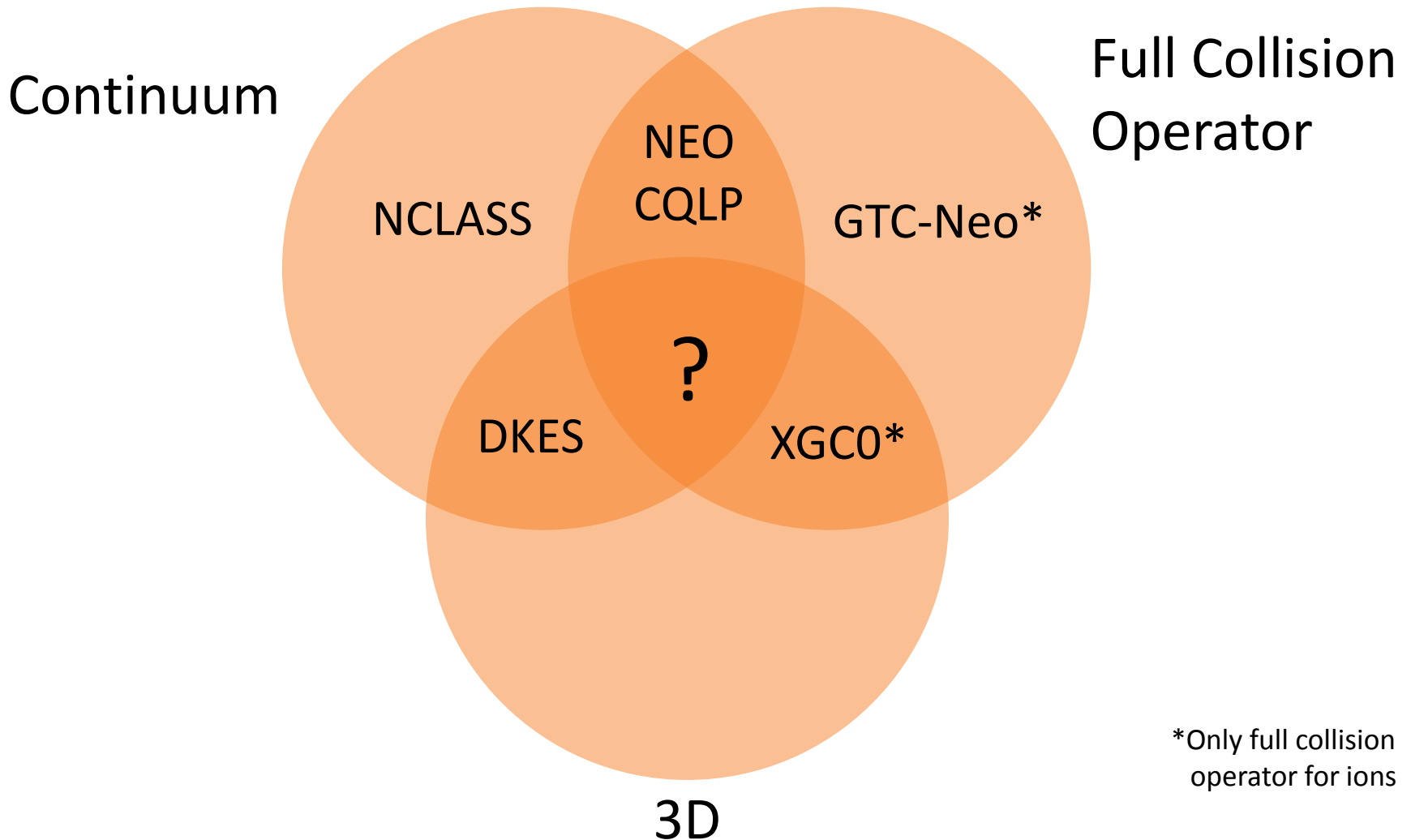
- Density, temperature, pressure, etc. tend to equilibrate across an island width
- Difference in current at O-point and X-point can drive island growth
 - ▣ Without these gradients, there can be no bootstrap current within the island
 - ▣ Bootstrap current at the X-point can drive island growth
- Large islands allow hot, dense plasma near core to be transported outward, reducing confinement
- Modifications to magnetic topology can result in macroscopic instability and disruption



Images taken from [The Theory of Toroidally Confined Plasmas](#) by R. White, 2006

Neoclassical code characteristics

25



Ramos DKE

26

$$\begin{aligned}
 & \frac{\partial f_{NM_e}}{\partial t} + \cos \chi \left(v \mathbf{b} \cdot \nabla f_{NM_e} + v_{the}^2 \mathbf{b} \cdot \nabla \ln n \frac{\partial f_{NM_e}}{\partial v} \right) - \frac{\sin \chi}{v} \left(v_{the}^2 \mathbf{b} \cdot \nabla \ln n - \frac{v^2}{2} \mathbf{b} \cdot \nabla \ln B \right) \frac{\partial f_{NM_e}}{\partial \chi} \\
 &= \left\{ \cos \chi \frac{v}{2T_e} \left(5 - \frac{v^2}{v_{the}^2} \right) \mathbf{b} \cdot \nabla T_e + \cos \chi \frac{v}{nT_e} \mathbf{b} \cdot \left[\frac{2}{3} \nabla (p_{e\parallel} - p_{e\perp}) - (p_{e\parallel} - p_{e\perp}) \nabla \ln B - \mathbf{F}_e^{coll} \right] \right. \\
 &+ P_2 (\cos \chi) \frac{v^2}{3v_{the}^2} (\nabla \cdot \mathbf{u}_e - 3\mathbf{b} \cdot [\mathbf{b} \cdot \nabla \mathbf{u}_e]) + \frac{1}{3nT_e} \left(\frac{v^2}{v_{the}^2} - 3 \right) [\nabla \cdot (q_{e\parallel} \mathbf{b}) - G_e^{coll}] \\
 &+ \frac{1}{6eB} \left[2P_2 (\cos \chi) \frac{v^2}{v_{the}^2} \left(\frac{v^2}{v_{the}^2} - 5 \right) + \frac{v^4}{v_{the}^4} - 10 \frac{v^2}{v_{the}^2} + 15 \right] (\mathbf{b} \times \boldsymbol{\kappa}) \cdot \nabla T_e \\
 &+ \frac{1}{6eB} \left[-P_2 (\cos \chi) \frac{v^2}{v_{the}^2} \left(\frac{v^2}{v_{the}^2} - 5 \right) + \frac{v^4}{v_{the}^4} - 10 \frac{v^2}{v_{the}^2} + 15 \right] (\mathbf{b} \times \nabla \ln B) \cdot \nabla T_e \\
 &\left. + P_2 (\cos \chi) \frac{v^2}{3eBv_{the}^2} (\mathbf{b} \times \nabla \ln n) \cdot \nabla T_e \right\} f_{M_e} + \langle C_{ee} + C_{ei} \rangle.
 \end{aligned}$$

with full Fokker-Planck-Landau collision operator

$$\begin{aligned}
 \langle C_{ee} + C_{ei} \rangle &= \nu_{De}(v) \mathcal{L}[f_{NM_e}] + \frac{\nu_e v_{the}^3}{v^2} \frac{\partial}{\partial v} \left\{ \xi_e \left[v \frac{\partial f_{NM_e}}{\partial v} + \frac{v^2}{v_{the}^2} f_{NM_e} \right] + \xi_i \left[v \frac{\partial f_{NM_e}}{\partial v} + \frac{m_e v^2}{m_i v_{thi}^2} f_{NM_e} \right] \right\} \\
 &+ \frac{\nu_e v_{the}}{n} f_{M_e} \left(4\pi v_{the}^2 f_{NM_e} - \Phi_e[f_{NM_e}] + \frac{v^2}{v_{the}^2} \frac{\partial^2 \Psi_e[f_{NM_e}]}{\partial v^2} \right) \\
 &+ \nu_e v_{the} f_{M_e} \left(\frac{T_e}{T_i} - 1 \right) \left[\frac{4\pi v_{thi}^2}{n} f_{Mi} - \frac{v}{v_{the}^2} \xi_i \right] + \nu_e f_{M_e} \frac{v_{the}}{v_{thi}^2} \frac{\mathbf{b} \cdot \mathbf{J}}{en} \xi_i \cos \chi,
 \end{aligned}$$

Nonaxisymmetric hybrid simulations

27

- Toroidal angle could be expanded in Fourier modes or finite elements
- No concentrically-nested flux surfaces
 - ▣ Flux surfaces still exist in most of torus, however, both inside and outside islands
 - ▣ May be possible to parameterize field lines or surfaces with something like (ψ, θ)
 - ▣ May require (R, Z) representation of poloidal plane

Possible nonaxisymmetric test case

28

- Begin with a stable equilibrium with a seed magnetic island
- Evolve equilibrium with neoclassical effects due to nonaxisymmetric code
- Explore how bootstrap current can destabilize the seed island, leading to neoclassical tearing mode